This is a repository copy of *Obtaining effective rate coefficients to describe the decomposition kinetics of the corannulene oxyradical at high temperatures*.

White Rose Research Online URL for this paper:
http://eprints.whiterose.ac.uk/115917/

Version: Accepted Version

Journal Name

ARTICLE

Obtaining Effective Rate Coefficients to Describe the Decomposition Kinetics of the Corannulene Oxyradical at High Temperatures

H. M. Wang,[ab] X. Q. You,[ab]* M. A. Blitz,[c] M. J. Pilling[c] and S. H. Robertson[d]*

Unimolecular reactions play an important role in combustion kinetics. An important task of reaction kinetic analysis is to obtain the phenomenological rate coefficients for unimolecular reactions based on the master equation approach. In most cases, the eigenvalues of the transition matrix describing collisional internal energy relaxation are of much larger magnitude than and well separated from the chemically significant eigenvalues, so that phenomenological rate coefficients may be unequivocally derived for incorporation in combustion mechanisms. However, when dealing with unimolecular reactions for a large molecule, especially at high temperatures, the large densities of states of the reactant cause the majority of the population distribution to lie at very high energy levels where the microcanonical reaction rate constants are large and the relaxation and chemical eigenvalues overlap, so that well-defined phenomenological rate coefficients cannot be determined. This work attempts to analyze the effect of overlapping eigenvalues on the high-temperature kinetics of a large oxyradical, based on microcanonical reaction rates and population distributions as well as the eigenvalue spectrum of the transition matrix from the master equation. The aim is to provide a pragmatic method for obtaining the most effective rate coefficients for competing elimination, dissociation, and bimolecular reactions for incorporation in combustion mechanisms. Our approach is demonstrated with a representative example, thermal decomposition and H addition reactions of the corannulene oxyradical.

1. Introduction

Unimolecular reactions play a major role in combustion. Relatively few rate coefficients have been determined experimentally,[1-5] and an important task in combustion kinetics studies is to obtain the reaction rate coefficients for such reactions by coupling electronic structure calculations and RRKM theory with the master equation (ME) approach, to determine the rate coefficients as a function of temperature and pressure. This theoretical approach has been shown to be accurate and effective.[6-13]

A ME model is constructed by dividing the vibration/rotation states of each participating molecule into a set of contiguous grains and describes the time evolution of the populations of these grains as a result of collisional energy transfer between the grains and microcanonical dissociation from them. One solution methodology uses a matrix approach, and the grain populations can be expressed using the eigenvalues and eigenvectors of the transition matrix which contains the first-order energy dependent collisional and reaction rate constants and operates on the grain population vector; the number of eigenpairs equals the number of energy grains. For a simple unimolecular dissociation (i.e., R→P), there is generally a single chemically significant eigenvalue (CSE) describing the chemical change; the rest of the eigenvalues are termed internal energy relaxation eigenvalues (IEREs) and they describe the relaxation of the population distribution to a pressure dependent steady state distribution. The IEREs are usually of much greater magnitude than the CSE, and this is a necessary condition for a phenomenological description of the chemical reaction in terms of the macroscopic rate law and the corresponding phenomenological rate coefficient $k(p,T)$,[8] as shown in Eq. 1.

$$\frac{d[P]}{dt} = -\frac{d[R]}{dt} = k(p,T)[R] \tag{1}$$

For a simple unimolecular dissociation, $k(p,T)$ is equal to the modulus of the CSE, $|\lambda_1|$, provided the CSE and IEREs are well separated. Miller et al.[12] in a comment on a paper by Barker et al.,[13] defined a phenomenological reaction as "an elementary reaction with ….its rate constant [that is] time-independent and [does] not depend on initial conditions over a very wide range of conditions…" For more complex reactions with multiple wells, the number of CSEs is equal to the number of wells plus the number of source terms. When using an eigenpair decomposition of the ME transition matrix, it is straightforward to obtain phenomenological rate coefficients for the component

[a.] Center for Combustion Energy, Tsinghua University, Beijing, 100084, China.
E-mail: xiaoqing.you@tsinghua.edu.cn
[b.] Key Laboratory for Thermal Science and Power Engineering of Ministry of Education, Tsinghua University, Beijing 100084, China
[c.] School of Chemistry, University of Leeds, Leeds, U.K.
E-mail: M.J.Pilling@leeds.ac.uk
[d.] Dassault Systèmes, BIOVIA, 334, Cambridge Science Park, Cambridge, U.K., CB4 0WN. E-mail: struanhrobertson@gmail.com

reactions if the CSEs are well separated from the IEREs.[8, 9] In this paper we consider reactions of large-molecules, which have large densities of states which cause the majority of population distributions to lie at very high energies,[14-23] especially at high temperatures, which gives rise to some unusual, but very interesting kinetic behavior. Firstly, the microcanonical reaction rate constants are so large that chemical reaction rates compete with, or even exceed, the rate of collisional relaxation. As a result, reaction, e.g. isomerisation or decomposition, can take place at a very early stage, independently of pressure. This effect can be detected by observing the relative magnitude of IEREs and CSEs, and by examining the population distributions and the microcanonical reaction rates. When eigenvalues overlap, it is impossible to obtain phenomenological rate coefficients as defined above. Specifically, for elimination or dissociation reactions without significant accumulation of intermediates, because several eigenmodes besides the CSE contribute to the time dependence of the reaction, the decays of the reactant are necessarily broader than a single exponential. As discussed above, the phenomenological rate coefficients cease to exist under this condition. Instead, we seek to determine what we will define as *effective rate coefficients* that can be used in combustion models. Inevitably, given the non-exponential time dependence, incorporation of such effective rate coefficients in combustion models carries a degree of approximation, as will be discussed below. Secondly, when other competing reactions are involved, because the evolution of the reactant cannot be fully represented by an effective rate coefficient, it is difficult to estimate correctly the branching ratios of the competing reactions using a conventional phenomenological model. It is therefore necessary to investigate the uncertainty of branching ratios caused by the use of effective rate coefficients.

This work attempts to perform a theoretical analysis on the time dependence of species concentrations at high temperatures for reactants with large densities of states, on the basis of microcanonical reaction rates, population distributions as well as the eigenvalue spectrum of transition matrix from the master equation, and provide a pragmatic method of obtaining the most effective rate coefficients for elimination or dissociation reactions. The modelling is aimed at a description of polycyclic aromatic hydrocarbon (PAH) and soot surface chemistry, where large molecules are involved at temperatures of 1500 – 2500 K. Our approach is demonstrated with a representative example, thermal decomposition and H addition reactions of the corannulene oxyradical. Firstly, the thermal decomposition kinetics of the corannulene oxyradical are studied by solving the master equation, with a focus on the effect of overlapping eigenvalues on the kinetic behavior. A number of ways of determining the effective rate coefficients are compared, and the accuracy of using thermodynamics to determine the reverse rate coefficients is examined and discussed. Secondly, the two competing reactions, thermal decomposition and H addition, of the corannulene oxyradical

are studied using the master equation approach to examine the interactions between these two reactions under conditions of eigenvalue overlap. Species concentration time profiles from the master equation modelling are compared with those from kinetic modelling with the effective rate coefficients.

2. Methodology

Based on the quantum-chemical results from our previous study,[22] the species concentration time evolution of the corannulene oxyradical reaction system was calculated for temperatures ranging from 1500 to 2500 K and pressures from 0.01-1000 atm by solving the master equation. The master equation code MESMER[10] was used for the calculations. MESMER[10] uses matrix techniques to formulate and solve the master equations for unimolecular systems composed of an arbitrary number of wells, transition states, sinks, and reactants. Microcanonical rate coefficients were computed using RRKM theory. Argon was chosen as the bath gas collider. The exponential-down model with a constant $\langle \Delta E \rangle_{down}$=260 cm^{-1} was used based on previous studies.[14-16, 18-20, 23] The Lennard-Jones parameters were estimated from an empirical correlation proposed by Wang and Frenklach.[24] A grain size of 100 cm^{-1} was chosen for the sake of both computational cost and accuracy.

The method of solution used in MESMER is based on the analysis of eigenpairs of the matrix describing reaction from and collisional energy transfer between the energy grains of the system. The phenomenological rate constants may be determined from the eigenvectors and eigenvalues obtained from the solution of the ME using an approach first discussed by Bartis and Widom,[25] and extended by Miller and Klippenstein[8, 9] and Robertson et al..[26] However, this approach only works when the IEREs are all well-separated in magnitude from the CSEs.[8, 9, 11] If this is not the case, then one approach is to fit the time-dependent species concentrations obtained from the ME to a phenomenological model and extract rate coefficients.[27] In the case of the oxyradical considered here, the CSEs are well separated from the IEREs only at lower (~1500 K)
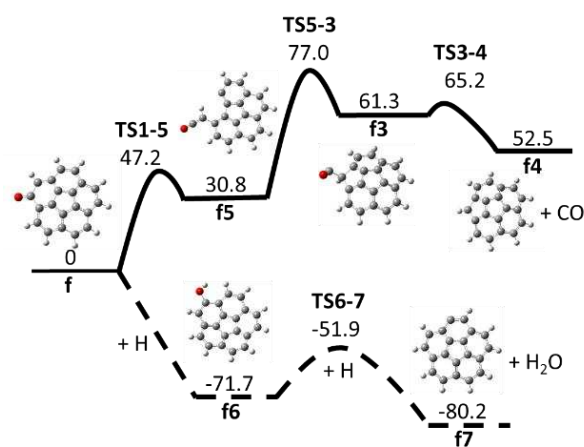

Figure 1 Potential energy surface of the decomposition and H addition reactions of corannulene oxyradical f at the B3LYP/6-311G(d,p) level at 0 K (units: kcal/mol)

but not at higher (~2500 K) temperatures as will be discussed later.

3. Results and discussion

3.1 Potential energy surface

Based on the chemical similarity approximation, corannulene may be taken to represent a graphene edge with a five-membered ring completely embedded in the edge, and the corannulene oxyradical is an intermediate in the oxidation process. Previous studies on soot surface chemistry[14-22, 28, 29] especially the kinetic Monte Carlo simulation studies by Singh et al. [29] revealed that there are two competing pathways of an oxyradical originating from soot surface oxidation. Fig. 1 presents the potential energy surface of two competing reaction pathways of the corannulene oxyradical at the B3LYP/6-311g (d,p) level. Note that, to be consistent, we have used a similar notation of molecules, radicals and transition states to that in our previous work.[23] As shown in Fig. 1, one pathway is the thermal decomposition of the corannulene oxyradical f, and the other is a barrierless hydrogen addition reaction to form intermediate f6, which may subsequently react with another H atom to produce the corannulenyl radical f7 and H_2O through TS6-7. The latter path regenerates the corannulenyl radical, instead of oxidizing it, therefore it will be referred to as the regeneration path.

3.2 Reaction kinetics

3.2.1 Species time profiles

The decomposition of corannulene oxyradicals f can be treated as a separate unimolecular reaction system, and we may obtain the species profiles, including only this path, using a master equation model. The master equation was initiated with a Boltzmann population of f, as f is an important intermediate

formed by oxidation reactions of OH or O_2 with the corannulene molecule; the Boltzmann population distribution in the reactant is likely to be retained in the product, given their molecular size. The bulk of the internal energy in the oxyradical resides in the vibrations associated with the ring structure and so will be little affected by any residual deviations from a Boltzmann distribution in the immediate vicinity of the newly formed oxyradical centre. It is important to stress, though, that this is an assumption, and the effective rate coefficients derived below are dependent on it. The results at 1 atm over the range 1500-2500 K are shown in Fig. 2, and those at other pressures can be found in Fig. S1 of the supporting information (SI). At 1500 K, almost all of the reactant (f) converts to product f4 on the timescale $10^{-5} - 10^{-2}$ s; at 2000 and 2500 K, f decays initially on a much shorter timescale ($10^{-11} - 10^{-10}$ s) to form intermediate f5. The concentrations of f and f5 remain almost constant until f4 is produced. The maximum concentration of f5 increases as temperature is increased, while there is no significant accumulation of intermediate f3 at all conditions; it reacts quickly by dissociation because of its shallow well. While reaction always proceeds via f5, its concentration at 1500 K is minimal, as noted above.

To examine the pressure dependence of the conversion from f to f5, the concentration ratios of f5 to f at 2500 K over 0.1-1000 atm are plotted in Fig. 3, and those at 2000 K are provided in Fig. S2 in the SI. The results reveal that there are apparently two reaction stages. In the first stage, f and f5 approach a steady state on a very short time scale (~10^{-10} s) with no pressure dependence. In the second stage, at pressures above ~100 atm, the concentration ratio of f5 to f increases with time and approaches a constant value, which corresponds to the equilibrium ratio. At lower pressures, the ratio decreases with time before becoming steady. To explain the results, the Boltzmann populations of f and f5 at 2500 K together with the microcanonical rate coefficients $k_{f-f5}(E)$ and $k_{f5-f}(E)$, are plotted
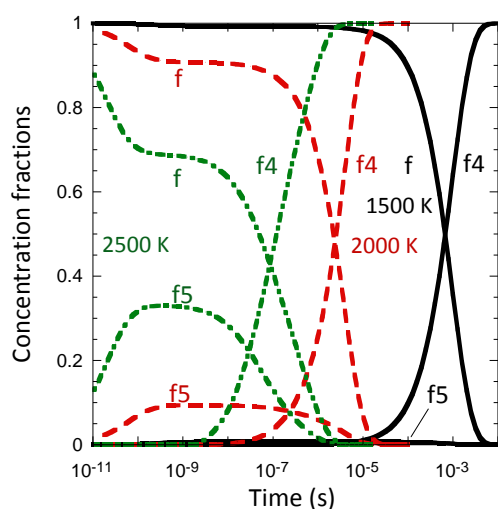

Figure 2 Species concentration profiles from the master equation modelling of corannulene oxyradical f decomposition at 0.1 atm, — 1500 K, --- 2000 K, ·— 2500 K.
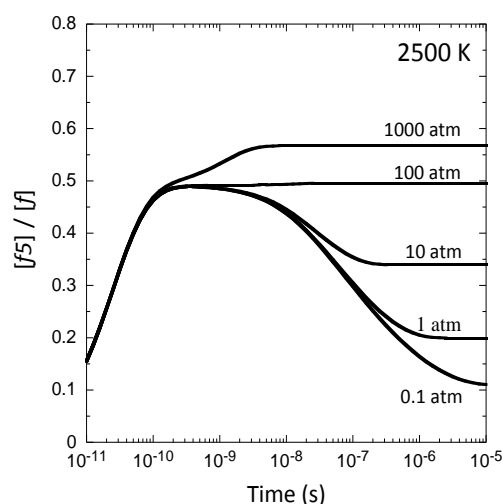

Figure 3 Concentration ratios of f5 and f from the master equation modelling of corannulene oxyradical f decomposition at 2500 K over 0.1 – 1000 atm
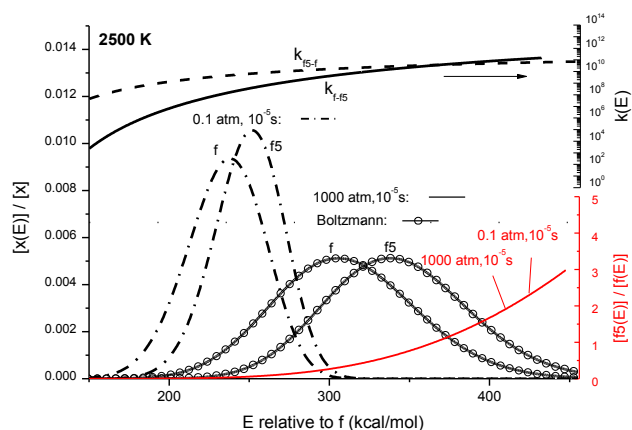
Figure 4 Boltzmann distribution of f and f5 at 2500 K; microcanonical rate coefficients of f and f5 isomerization; concentration distributions of f5, f, and their ratios over energy from the master equation modelling of corannulene oxyradical f decomposition at 10^{-5} s, 2500 K and at 0.1 and 1000 atm.
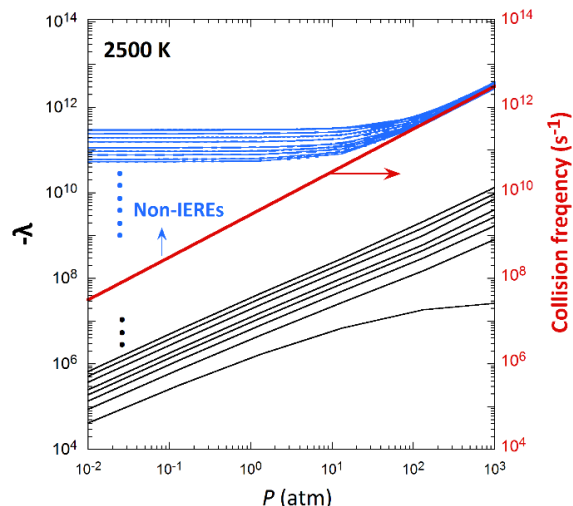

Figure 5 The eigenvalue spectrum and collision frequency from the master equation modelling of corannulene oxyradical f decomposition as functions of pressure at 2500 K.

in Fig. 4. The master equation was initiated with a Boltzmann population distribution for f. Fig. 4 shows that the maximum population lies at ~300 kcal/mol and the fraction of the population below the potential energy of the transition states TS1-5 and TS5-3 is minimal. As $k_{f-f5}(E)$ and $k_{f5-f}(E)$ at the peaks of the Boltzmann distributions of f and f5 are larger than 10^{10} s^{-1}, f and f5 isomerize rapidly and the collision frequency is too small at these short time scales to produce significant relaxation. It is noteworthy that, although f5 has a higher potential energy than f, the equilibrium concentration of f5 is substantial, due to its smaller vibrational frequencies. To explain the trends of the second stage in Fig. 3, Fig. 4 presents the populations of f and f5 and the energy-dependent concentration ratios of f5 to f at two extreme pressures, 0.1 and 1000 atm, at a typical time scale of the second stage of reaction of 10^{-5} s. We can see that the concentration ratio (red lines) does not depend on pressure; the two red lines are indistinguishable, but increase with energy, which indicates that, at every energy level, these two species reach "microcanonical equilibrium" rapidly regardless of the pressure. However, at lower pressures, the majority of the distributions of f5 and f shift towards lower energy states due to the more extensive reactive depletion of f5 and f (which behave almost as a single reactant) at higher energies. Because $[f_5(E)]/[f(E)]$ is smaller at these lower energies, the ratio of the overall species concentration approaches a steady state smaller than the canonical equilibrium ratio. The canonical equilibrium can only be reached at very high pressures where collisional energy transfer is sufficient to suppress the shift of distributions, while at lower pressures, where the collision frequency is insufficient to repopulate f (and therefore f5) at higher energy levels, these levels have negligible population since the depletion is faster than the collisional relaxation.

3.2.2 Eigenvalue spectrum

The fast isomerization between f and f5 at high temperatures can be examined not only from the population distributions and the microcanonical reaction rates, but also from the behavior of the IEREs and CSEs. Figure 5 shows the pressure dependence of a band of eigenvalues at 2500 K spanning the range $10^4 – 10^{12}$ s^{-1}, along with the inelastic collision frequency calculated by MESMER, which is conventionally assumed to be the same as that experienced by molecules subject to a Lennard-Jones potential. At low pressures the eigenvalues of largest magnitude ($10^{10} – 10^{12}$ s^{-1}) are independent of pressure, but become pressure dependent at higher pressures. As we know, IEREs depend linearly on the collision frequency. The low-pressure eigenvalues in this range are, therefore, not IEREs, but relate to the microcanonical reversible isomerization between f and f5. Each pair of isoenergetic grains between the two isomers equilibrates, but evolves independently of those at
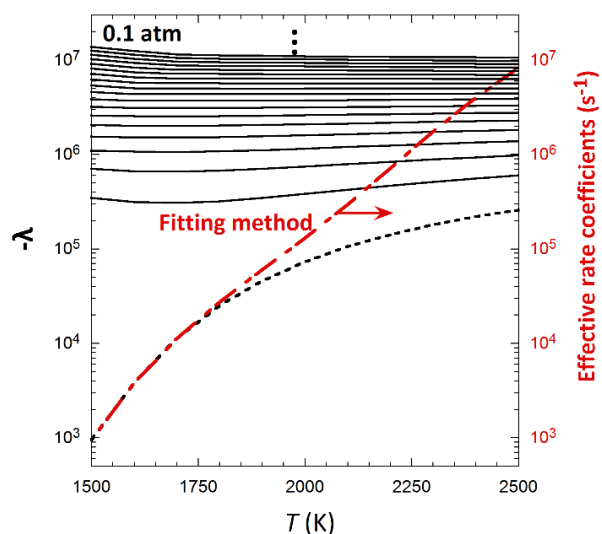

Figure 6 The eigenvalue spectrum and the effective rate coefficients obtained by optimal fitting method from the master equation modelling of the reduced system of corannulene oxyradical f' decomposition at 0.1 atm over 1500-2500 K.

other energies. As discussed in appendix A, the eigenvalues of a pair of grains are zero and $-(k_{f\text{-}f5}(E) + k_{f5\text{-}f}(E))$ and so there are as many reactive eigenvalues as there are grain pairs contributing to the isomerization. The time dependence of the overall isomerization is, therefore, non-exponential as shown in Fig. S3 in the SI. As the pressure increases, the IEREs begin to overlap with these reactive eigenvalues and the process becomes more complex, with partial collisional relaxation in the two isomers competing with isomerization. Consequently, the concentration ratio of f5 to f increases with time and becomes constant at pressures above 100 atm at 2500 K as shown in Fig. 3. However, at lower temperatures, say 2000 K, this process occurs at lower pressures (10 atm, see Fig. S2 in the SI), and both the contribution of f5 to the overall process and its equilibrium concentration fall as the temperature is reduced.

This type of behaviour, with the largest magnitude eigenvalues showing pressure independence at low pressures, was discussed many years ago by Pritchard[30] for model systems. It occurs in all master equation calculations which include high energy grains with large microcanonical rate coefficients. In most cases, the behaviour has no practical significance because the population of those grains is negligible. The difference in the present case arises because of substantial population of the high energy grains with large microcanonical rate coefficients. It is expected that both the high temperature and the large densities of states resulting from the size of radicals, coupled with the low threshold energy for isomerization, have an effect on this type of eigenvalue behaviour. The SI shows a comparison of the Boltzmann distributions and microcanonical rate coefficients at 1500 - 2500 K for another two radicals which are different in size, phenoxy [19] and a large condensed ring oxyradical, g, derived from our earlier work. [23] This series of calculations, discussed in greater detail in the SI, shows the effect of molecular size and temperature on kinetic behaviour.

The short timescales on which this complex process of local equilibration and collisional relaxation occurs mean that it is unlikely to be overlapped by, or in competition with, reactive processes of importance in combustion. It is not necessary,

therefore, to attempt to represent the kinetics of the process in a combustion model. Miller and Klippenstein[11] proposed a general species reduction method to handle the situation when a CSE merges with the IEREs by combining the two species that are equilibrated through the chemical reaction eigenmode into a single species. Similar to this methodology, as demonstrated in these calculations, we can represent f and f5 as a single species f' containing grains with numbers of states in a grain equal to the sum of states of the two species. Reaction to form f3 has microcanonical rate constant expressions containing the sum of states already calculated for $k_{f5\text{-}f3}$ and an appropriate density of states, as discussed in the SI. Figure S1 in the SI shows the species profiles determined from master equation modelling of the reduced system after the species reduction (referred to as the reduced system hereafter), which shows the formation of f4 and CO mirrors the decay of reactant f' in the reduced system and the formation of intermediate f3 is negligible due to its very shallow well. The reduced system well reproduces the species time evolution at longer time scales compared to the complete system.

Note that in this representation, the reduced system is, in effect, a simple dissociation reaction. Figure 6 shows the eigenvalue spectrum (black lines) as a function of temperature at 0.1 atm. It is generally accepted that, for a dissociation reaction with a CSE well-separated from the IEREs, the rate coefficient for formation of CO is equal to the modulus of the smallest magnitude eigenvalue, as in the case of 1500 K. However this is not the case at higher temperatures where overlap is significant and the smallest eigenvalues are insufficient to describe the reactive step even when f and f5 are combined. Because several eigenmodes contribute, the decay of the reactant and the production of CO extend over several decades in time, indicating that the process is non-exponential and a simple first order rate coefficient cannot be assigned. This is confirmed by Fig. S4 in the SI which shows a ln([f']) vs. time plot and demonstrates considerable curvature i.e. non-exponential behaviour, so that a direct determination of the rate coefficient is problematic.
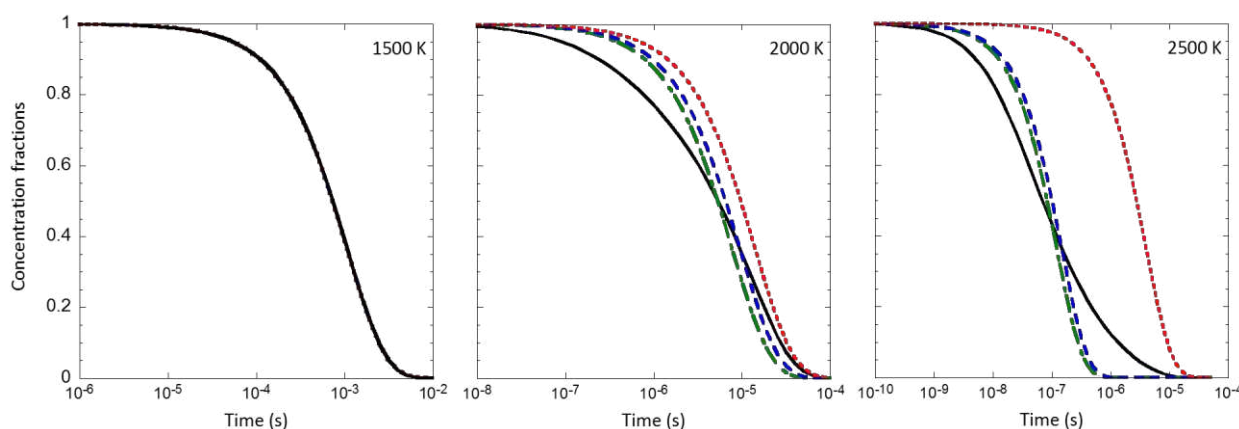

Figure 7 Comparison of species concentration profiles of f' at 0.1 atm from the master equation modelling of the reduced system of corannulene oxyradical f' decomposition with those from the fitting formula *exp(-kt)* where *k* is the effective rate constant derived from three different methods. — master equation modelling, -- - 1/e method, ·— fitting method, ·····eigenvalue method.

3.2.3 Effective rate coefficients

As discussed in the last section, the phenomenological rate coefficient cannot be obtained from the eigenvalue of the smallest magnitude except at 1500 K. In this section, we shall discuss a few ways to determine the *effective* rate coefficients from the species time profiles to which several eigenmodes contribute. The aim is to provide an appropriate parameter that will provide the best representation of the dissociation kinetics in a combustion mechanism. The first one is called the optimal fitting method: the effective rate coefficient is equated to the slope from fitting $\ln([f'])$ vs. time, where $[f']$ is the concentration of the reactant in the reduced system. By varying the concentration or time range for fitting, we may minimize the sum of squares of deviations $\sum_{\text{time}}([f'] - [f']_{\text{fitted}})^2$ and obtain the optimal concentration or time ranges. The second one is called the eigenvalue method, which uses the absolute value of the lowest magnitude eigenvalue as the rate coefficient. The third one is called the 1/e time method, which equates the rate coefficient to the reciprocal of time at which $[f']$ is equal to 1/e.

Figure 7 shows the comparison of concentration profiles of the reactant from the master equation modelling with those from the fitting formula e^{-kt}, using the three different methods to calculate k over the range 1500-2500 K at 0.1 atm, where k is the effective rate coefficient. As can be seen, at 1500 K, the species profiles from the fitting formula e^{-kt} are almost identical to those from the master equation modelling, while they differ from each other at 2000 and 2500 K. Among the three methods, both the optimal fitting and the 1/e time methods produce concentration profiles closer to the master equation modelling results than the eigenvalue method, and the optimal fitting method is the best. Figure 7 demonstrates the highly non-exponential decays at the higher temperatures and shows that the effective rate coefficients generate decays that necessarily overestimate $[f']$ at short times and underestimate it at long times. The comparison of the effective rate coefficients obtained by the optimal fitting method with the eigenvalue spectrum at 0.1 atm can be seen in Fig. 6. The comparison at other pressures can be found in Fig. S6 in the SI. It is noted that the effective rate coefficient is identical to the numerically smallest eigenvalue at low temperatures, consistent with previous observations. However, at high temperatures the effective rate coefficient is much larger than the eigenvalue of smallest magnitude, and falls well within the IERE continuum. Under these high temperature conditions, as is clear from Fig. 7, several eigenmodes contribute to the decay of reactant and the separation of the eigenvalue spectrum into IERE and CSE terms is no longer meaningful. It is also noteworthy that the temperature at which the effective rate coefficient differs from the smallest eigenvalue increases with pressure as shown in Fig. S6.

Figure 8 shows the temperature dependence of the effective rate coefficients generated by the three different
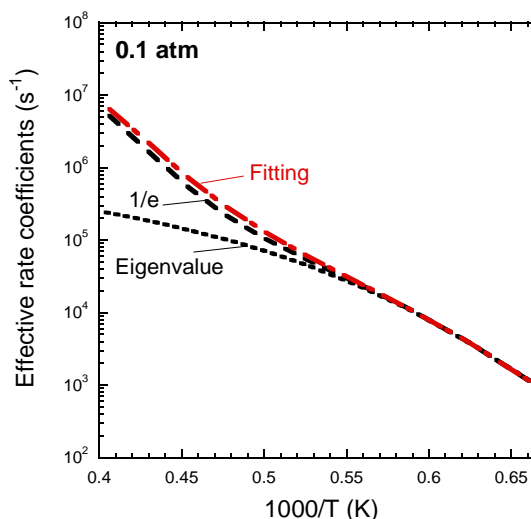

Figure 8 Temperature dependence of the rate coefficients of the reduced system of corannulene oxyradical f' decomposition over 1500-2500 K at 0.1 atm. --- 1/e method, ·— fitting method, ·····eigenvalue method.

methods at 0.1 atm. The comparisons at other pressures can be found in Fig. S5 in the SI. It is worth noting that the effective rate coefficients show different temperature and pressure dependences. For the eigenvalue method, the pressure dependence of rate coefficients is more significant as temperature is increased; however, for the 1/e time and the optimal fitting methods, the most significant pressure dependence occurs around 2000 K (see Fig. S5). This is apparently due to the increasingly non-exponential character of the time dependence of the concentration profiles at higher temperatures. Using the lowest magnitude eigenvalue as the effective rate coefficients would severely underestimate the fast decay of the concentration profiles due to the mixing of eigenmodes whose corresponding eigenvalues extend the loss of f' to significantly shorter times.

It is important to emphasize that this problem of CSE / IERE overlap cannot be accommodated by combining species to eliminate the overlap, as was possible for the isomerization reaction discussed above, and as was examined in detail by Miller and Klippenstein.[11] Dissociation is the sole remaining process in the reaction, which is now a single species system. The highly non-exponential behavior cannot be eliminated; we have chosen to provide a necessarily approximate description for incorporation in combustion models, in which an exponential decay, with an associated time independent rate

Table 1 Comparison of the forward and reverse rate coefficients of the reduced system of corannulene oxyradical f' decomposition obtained by different methods.

0.1 atm	T (K)	1500	2000	2500
k_f	Method I	9.4×10^2	1.3×10^5	8.3×10^6
(s^{-1})	Method II	9.4×10^2	1.1×10^5	6.9×10^6
k_r	Method I	3.4×10^7	1.0×10^8	9.9×10^8
(cm^{3}mol^{-1}s^{-1})	Method II	3.4×10^7	1.0×10^8	1.4×10^9

coefficients, has been determined to represent this multiexponential decay. The associated inaccuracy raises questions about the validity of the determination of the reverse rate coefficients and the kinetic representation when the reaction competes with, or is associated with, other reactions. This question is examined in the following sections.

3.3 Reverse rate coefficients

As discussed above, the effective rate coefficients for f' dissociation are only representative of the non-exponential decay of f', which are compromised by the overlap between IEREs and CSEs, especially at higher temperatures. Thus the use of thermodynamics to determine the reverse rate coefficient based on these decomposition effective forward rate coefficients is questionable and needs to be examined because of the complex nature of the decomposition reaction and the contribution of several eigenmodes to it. In the following we shall discuss two different ways of determining the reverse rate coefficients, and then test them by examining the master equation under reversible conditions. We will compare the concentration profiles obtained from kinetic modelling of f' ⇌ f4 + CO using effective forward and reverse rate coefficients derived by different methods. In the present case, master equation modelling under reversible conditions means that the final step forming CO is made reversible with a fixed concentration of CO. For a well-behaved system, this results in two CSEs, one of which is zero.

The effective forward and reverse rate coefficients for kinetic modelling were derived in two different ways. One is by use of thermodynamics; in other words, the non-reversible master equation was solved and the optimal fitting method was used to determine the forward effective rate coefficient k_f, and the reverse rate coefficient k_r was determined from k_f divided by equilibrium constant K_c. The other uses the relaxation time constant by performing the reversible master equation modelling with different CO concentrations and deriving the reciprocal of time for each run, at which $([f']-[f'_{eq}])/(1-[f'_{eq}])$ equals $1/e$, where $[f'_{eq}]$ is the concentration fraction of f' at equilibrium, and equating this to k_{rel}. k_{rel} is called the relaxation

time constant, which is formally equal to $k_f + k_r[CO]$. A plot of the linear relationship of $k_f + k_r[CO]$ vs. [CO] was used to determine k_f and k_r. A total of 18 runs was carried out with different CO concentrations that vary from 10^{14} to 10^{17} molecule/cm^3. Table 1 compares k_f and k_r obtained by the relaxation time constant method (Method II) and those from the thermodynamics method (Method I). The two methods produce almost identical results of k_f and k_r at 1500 and 2000 K. However, because of the stronger overlap of CSEs and IEREs, k_r calculated by the relaxation time constant method is around 35% larger than that of the thermodynamics method at 2500 K, and thus both K_c and the equilibrium concentration of f4, $[f4_{eq}]$, are also underestimated.

One of the problems in this analysis is that the concentration of f' at equilibrium is very small: at accessible [CO], the reaction is essentially irreversible. Using an extremely large CO concentration, $[CO] = 10^{17}$ molecule/cm^3, we compared the species profiles from the master equation modelling with those from the kinetic modelling in which the rate coefficients were computed from the thermodynamics method. As shown in Fig. 9, the ME and kinetic modelling give almost identical concentration profiles at 1500 K, which is reasonable since the IEREs and CSEs do not overlap badly. By contrast, above 2000 K, the kinetic modelling underestimates the changing rate of species concentration predicted by the master equation modelling at shorter times, but overestimates it at longer times.

As noted above, the equilibrium constant is such that, even with an inaccessible $[CO] = 10^{19}$ molecule cm^{-3}, the equilibrium is well over to f4+CO at temperature above 2000 K and the effective pseudo first order rate constant for the reverse reaction is much smaller than that for the forward reaction. To test the effects of non-exponential approach to equilibrium more fully, a model system was examined in which the product energy was increased by 25 kcal mol^{-1}. The results are presented in the SI. They show that the two approaches for determining the reverse rate coefficient differ by nearly 40% at 2500 K. As expected, the thermodynamics method reproduces the final yields obtained from the master equation more closely than does the relaxation method (see Fig. S7 in the SI). Since the relaxation method underestimates the yields, we have also
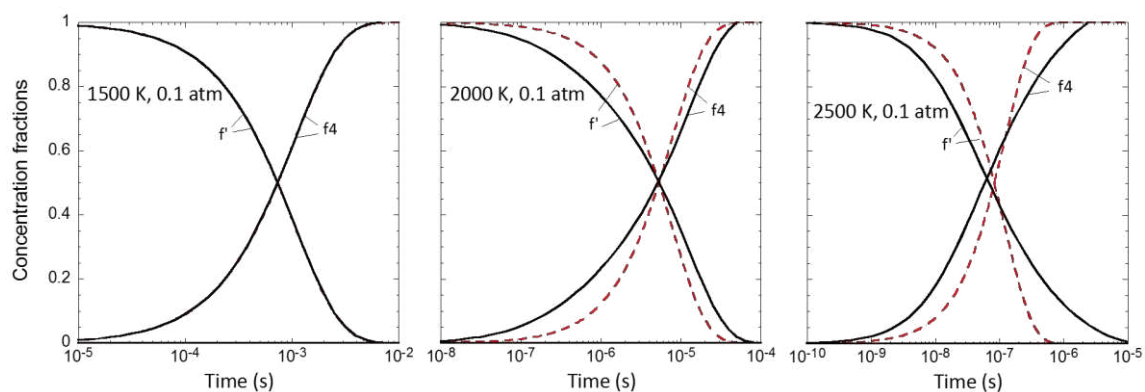

Figure 9 Species profiles of the reduced system of corannulene oxyradical f' decomposition over 1500-2500 K at 0.1 atm, [CO] = 10^{17} molecule cm^{-3} — reversible master equation modelling, --- kinetic modelling based on the thermodynamics method.

performed a combined method for determining k_f and k_r from k_{rel}. At a given concentration of [CO], k_f and k_r are obtained by maintaining the ratio of k_f and k_r at the value determined by K_c. This combined method generates slightly larger k_f than the two methods mentioned above as shown in the SI.

These calculations demonstrate that, although accuracy is impaired at the 2500 K, using thermodynamics to calculate the reverse from the forward rate constant provides satisfactory results, within the obvious constraints of the non-exponential behaviour discussed in the previous section.

3.4 Competing reactions

The overlap of the eigenvalues not only complicates the determination of effective forward and reverse rate coefficients, but also potentially affects the competition among reaction pathways of corannulene oxyradicals. Master equation modelling was performed for the two-pathway system shown in Fig. 1, assuming the mole fraction of H to be 0.01 at 1 atm. The reaction f + H → f6, hydrogen addition to the corannulene oxyradical, is a barrierless reaction, for which the inverse Laplace transform (ILT) method was utilized to obtain the microcanonical reaction rate constants. The canonical rate coefficient provided for ILT was estimated to be the same as that of the analogous reaction of phenanthrene oxyradicals, around 4×10^{-10} cm³molecule⁻¹ s⁻¹ at 1500-2500 K, based on the study of Edwards et al.[21,22] The reaction f6 ↔ f + H, was treated as a reversible dissociation reaction where the partitioning of energy between the dissociated products f and H is assumed to be statistical, that is the energy distribution of species f, on dissociation of f6 is the prior distribution.[31, 32] Here the probability of species f formed with energy E, $P(E|E_x)$, is given by Eq. 2:

$$P(E|E_x) = \frac{\rho_f(E)\rho_t(E_x - E)}{\rho_f \otimes \rho_t(E_x)} \qquad (2)$$

where E_x is the energy available to the dissociated products f and H. ρ_f is the ro-vibrational density of states of f; ρ_t is the relative translational density of states of the f and H fragments and is modelled using a classical expression *i.e.*, $\rho_t \propto \sqrt{E_t}$, where E_t is the relative translational energy, and $[\rho_f \otimes \rho_t]$ represents a convolution. It is clear that detailed dynamical calculations are required in order to investigate the general form of the product energy distribution. However, as the bulk of the internal energy in the oxyradical resides in the vibrations associated with the ring structure, statistical partitioning is assumed here as a first approximation. The distribution of f is also affected by dissociation via f5, as discussed above, and the influence of both of these processes (dissociation of f6 to form f and dissociation of f via f5) are accommodated within the formulation of the master equation. Dissociation of f6 to form the products involves addition of H followed by dissociative loss of H_2O to regenerate corannulene, i.e. f6 + H → f7 + H_2O. Thus

Table 2 The ten lowest magnitude eigenvalues from master equation modelling of the two-pathway system in Fig. 1 and the reciprocal characteristic times of product formation (the time when the mole fractions of products reach the half of their maximum values).

2500 K			
P (atm)	Eigenvalues (s⁻¹)	1/Time at [product]$_{max}$/2 (s⁻¹)
10^{-1}	-1.80x10⁷, -1.75x10⁷, -1.70x10⁷, -1.65x10⁷, -1.60x10⁷, -1.56x10⁷, -1.52x10⁷, -1.47x10⁷, -1.41x10⁷, -1.34x10⁷	f4	4.90x10⁷
		f7	2.35x10⁷
10	-2.14x10⁸, -1.88x10⁸, -1.62x10⁸, -1.38x10⁸, -1.14x10⁸, -9.21x10⁷, -7.13x10⁷, -5.18x10⁷, -3.39x10⁷, -1.77x10⁷	f4	4.07x10⁷
		f7	2.72x10⁷
2000 K			
P (atm)	Eigenvalues (s)	1/Time at [product]$_{max}$/2 (s⁻¹)
10^{-1}	-1.76x10⁷, -1.74x10⁷, -1.68x10⁷, -1.63x10⁷, -1.59x10⁷, -1.54x10⁷, -1.50x10⁷, -1.46x10⁷, -1.41x10⁷, -1.34x10⁷	f4	2.26x10⁷
		f7	2.00x10⁷
10	-2.27x10⁸, -1.94x10⁸, -1.64x10⁸, -1.36x10⁸, -1.11x10⁸, -8.85x10⁷, -6.71x10⁷, -4.73x10⁷, -2.95x10⁷, -1.40x10⁷	f4	1.94x10⁷
		f7	2.03x10⁷

the distribution of f6 is determined by its nascent distribution, following association of f and H, by collisional relaxation and by reaction with H. The reaction with H proceeds via a well-defined transition state and the product was treated as a bimolecular sink in the ME modelling, using the method discussed in Ref.[33], with microcanonical rate constants determined using RRKM theory. Under the conditions studied, this reaction occurs rapidly with the products effectively formed directly from f with no accumulation of f6. The species profiles from master equation modelling at 1500-2500 K and 0.1-10 atm are shown in Fig. 10. The eigenvalues and reciprocal characteristic times of product formation at 2000 and 2500 K are compared in Table 2. At lower temperatures, the regeneration pathway is dominant over the thermal decomposition pathway, while, at high temperatures, the latter becomes more competitive. As pressure is increased, the dominance of the decomposition pathway increases, and this dominance becomes even more significant at higher temperatures. The temperature and pressure dependence is a result of thermal decomposition being a higher activation-energy process than regeneration, and very frequent collisions with the bath gas are required to maintain the population of the high energy states needed for dissociation at the higher temperatures.

Finally, the competition between the decomposition and regeneration pathways for the reduced system was examined using a kinetic model with two phenomenological reactions, f' → f4+ CO and f' $\xrightarrow{+H}$ f6 $\xrightarrow{+H}$ f7+ H_2O and the species profiles from the kinetic modelling were compared with those from the master equation solutions for the two-pathway system. Note that to reveal the influence of the time dependence of the rates on the competition between the decomposition and regeneration pathways, the phenomenological rate coefficients of the two pathways were obtained separately from the master equation modelling with the individual pathways. In other words, the effective rate coefficient of the decomposition reaction, f' → f4+ CO, was obtained by optimal fitting of the f' decay profile computed by the master equation modelling with only the decomposition pathway (reduced system). The regeneration reaction $\mathbf{f'} \xrightarrow{+H} \mathbf{f6} \xrightarrow{+H} \mathbf{f7 + H_2O}$ was treated as a pseudo first-order reaction $\mathbf{f'} \xrightarrow{+2H} \mathbf{f7 + H_2O}$, with rate $k_{f\text{-}f6}$[H],
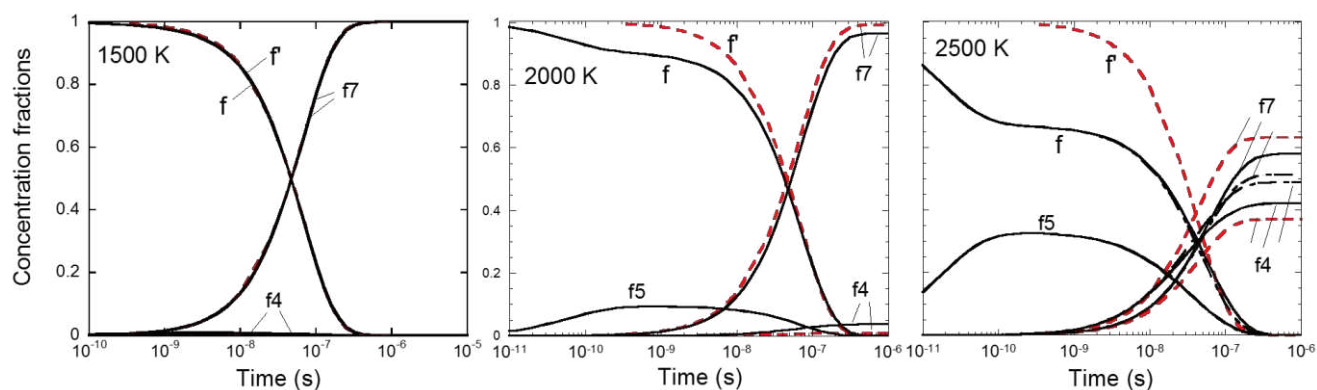
Figure 10 Comparison of the master equation modelling of the two-pathway system in Fig. 1 with the kinetic modelling results in which the phenomenological rate coefficients were obtained from master equation modeling of two single-pathway systems separately over 1500-2500 K and 0.1-10 atm. — ME modelling at 0.1 atm, - — ME modelling at 10 atm, --- kinetic modelling at 0.1 atm.

since the concentration of f6 is in steady state. The rate coefficients were obtained by linear fitting of [f] from the master equation modelling with only the regeneration pathway system. As shown in Fig. 10, compared to the master equation modelling results of the two-pathway system, the concentration profiles from the kinetic modelling are almost identical at 1500 K, however, as temperature is increased, the branching ratios of the decomposition reaction and the characteristic time of product formation (f4 + CO) predicted by the kinetic modelling are underestimated by as much as 30 % at 2500 K, 0.1 atm. The underestimation is suppressed at higher pressures, say 10 atm. As discussed earlier, the majority of the corannulene oxyradical population lies at very high energy levels above the transition states initially, but the depletion of f to produce f4 makes the distribution shift to lower energy levels at longer times as a result of insufficient repopulation, which causes the decomposition reaction rates to decrease with time. At high temperatures and low pressures, the decomposition pathway at short time scales is more significantly underestimated by the phenomenological model. Hence, to reduce the uncertainty, the effective rate coefficients should be derived from the decay of f' and the product yields computed by master equation modelling with the two-pathway system rather than the two single pathway systems.

4. Summary

In this work, we performed a theoretical analysis of the (i) isomerization and (ii) decomposition of the corannulene oxyradical at high temperatures, on the basis of microcanonical reaction rates, population distributions and the eigenvalue spectrum of the transition matrix from the master equation, and provided a pragmatic method for obtaining the most effective rate coefficients for decomposition. The reaction system shows interesting properties that derive from the size of the reactant and the high temperature.

(i) The distribution of the initial reactant was assumed Boltzmann which results in the bulk of the reactants having energies well in excess of the isomerization threshold. As a

result, most of the microcanonical rate coefficients exceed the collision frequency at all but the highest pressures and isomerization occurs without collisional relaxation; the largest magnitude eigenvalues relate to microcanonical isomerization and exceed the internal energy relaxation eigenvalues. Comparison with the behavior of other radicals in the SI shows that this effect is a result of the size of the reactant, the high temperature, and the low isomerization threshold. The problem of representing this process in a kinetic model was overcome by merging the states of the two isomers in a species reduction process.

(ii) There is considerable overlap between the IEREs and the chemically significant eigenvalue for dissociation. As a result the decay of the reactant and the formation of the products are highly non-exponential. This effect was again shown to be a consequence of the high temperature and is exacerbated by the size of the reactant. The problem cannot be resolved by species reduction, since this is the sole remaining reaction. We discussed three ways to determine the effective rate coefficients for dissociation based on an analysis of the time profiles of the reduced system. We found that the optimal fitting method produced concentration profiles closest to the master equation modelling. The effective rate coefficients obtained from different methods also demonstrate significantly different pressure dependences. We used the thermodynamics method and the relaxation time constant method to determine the reverse rate coefficients, and examined the influence of the time dependence on the reverse rate coefficients so obtained. The results show that the two methods give almost identical results at 1500 and 2000 K. However, at 2500 K, due to the strong overlap of the CSEs and IEREs, the reverse rate coefficients calculated by the relaxation time constant method are around 35% larger than that of the reversible method, leading to a lower apparent equilibrium constant. Finally, species time evolutions were examined for two competitive pathways, and the results show a maximum 30% difference between the master equation modelling results of a two-pathway system and those of the kinetic modelling with phenomenological rate coefficients obtained from master equation modeling of two single pathway systems. We also note

that the overlap of eigenvalues and hence the time-dependence of rate coefficients are sensitive to the energy transfer model applied in the master equation modelling. In the current case, specifically, applying a larger value of $\langle \Delta E \rangle_{down}$, the time dependence of rate coefficients becomes weaker. Further investigation of the energy transfer parameters of large PAHs colliding with bath gases will be reported in a future publication.

It is important to emphasize that the non-exponential character of the time profiles in these reactions is intrinsic to the system and stems from the high temperatures and the very high densities of states and depends on the initial Boltzmann distribution which in turn leads to high microcanonical rate coefficients in regions of high population and to the magnitudes of the eigenvalues associated with reaction exceeding or overlapping with the IEREs. Indeed, at high temperatures there is a manifold contribution of terms to the decay and the distinction between IERE and CSE eigen terms is no longer meaningful. While the problems of large microcanonical rate constants for isomerization could be overcome by species reduction, the effects of eigenvalue overlap on dissociation cannot be mitigated by the combining of species that has proved effective elsewhere:[11] dissociation of the reduced system based on the combination of f and f5 still generates non-exponential kinetics at high temperatures.

It is also noteworthy that our work is largely at an exploratory stage of studying the non-exponential decomposition behaviour of these large molecules, but the representational methodology would work for any simple decomposition reactions where CSEs and IEREs overlap, and where the effects cannot be mitigated by species reduction. The problem of assessing the impact of the representation of the kinetics of such a system on the modelling of interacting chemical reactions needs further investigation. We have made a preliminary analysis for simple reversible and coupled reactions in the latter part of this paper. Further analysis, including the investigation of a more formal description, is required.

Acknowledgements

Dedication

This paper is dedicated to the memory of Professor Ian W M Smith.

Appendix

In this appendix the extreme low pressure limit of the eigenvalue spectrum of the ME transition matrix is examined.

First, consider the case of a simple dissociation reaction, the transition matrix for such a system is:

$$M = \omega(P - I) - K \quad (1)$$

where ω is the collision frequency, P is the collision transition probability matrix, I is the identiy matrix and K is a diagonal matrix with the grain microcanonical rate coefficients on the diagonal. As the pressure declines $\omega \to 0$ so that $M \to -K$. As K is already diagonal then it follows directly that the eigenvalues of M, at low pressure, are zero below the threshold and equal to the grain microcanonical rates above the threshold. This was observed by Pritchard.[28] These eigenvalues will start to appear as ω becomes less than the individual $(K)_{ii}$ elements (i.e. not at the same pressure).

For isomerization the situation is a little more complex. Consider the reaction $A \rightleftharpoons B$ In this case we can write the transition matrix as,

$$M = \begin{pmatrix} \omega_A(P_A - I) - K_{BA} & K_{AB} \\ K_{BA} & \omega_B(P_B - I) - K_{AB} \end{pmatrix} \quad (2)$$

Again as the pressure drops $\omega_A \to \omega_B \to 0$ and the transition matrix takes on the form:

$$M \to \begin{pmatrix} -K_{BA} & K_{AB} \\ K_{BA} & -K_{AB} \end{pmatrix} \quad (3)$$

To make progress here it is noted that the eigenvalues of the transition matrix are not affected by a permutation of the rows and columns. In this way we can gather together all terms associated with a pair of iso-energetic grains, and when we do this we end with a block diagonal matrix, each block being a two-by-two matrix. These two-by-two matrices govern the exchange between iso-energetic states (grains) of the isomers, they can be individually diagonalized and each gives a zero eigenvalue (which follows from detailed balance) and a eigenvalue which is the negated sum of the forward and reverse microcanonical rate coefficients. From this it follows that there will be a set of eigenvalues that will start to appear when $\omega_A < K_{BA}$ and $\omega_B < K_{AB}$, and that their number will be the number of grains above the threshold.

In this region the system is reaching a microcanonical "equilibrium" through vibrational energy redistribution, but, because it is decoupled from the collisional heat bath, it does not reach a canonical "equilibrium". For this reason the definition of a canonical rate coefficient is problematic under these circumstances.

References

1. V. Vasudevan, D. F. Davidson and R. K. Hanson, *J. Phys. Chem. A*, 2005, **109**, 3352-3359.
2. K. W. McKee, M. A. Blitz, P. A. Cleary, D. R. Glowacki, M. J. Pilling, P. W. Seakins and L. Wang, *J. Phys. Chem. A*, 2007, **111**, 4043-4055.
3. M. J. Pilling, *Proc. Combust. Inst.*, 2009, **32**, 27-44.

4.   M. Teresa Baeza-Romero, M. A. Blitz, A. Goddard and P. W. Seakins, *Int. J. Chem. Kinet.*, 2012, **44**, 532-545.

5.   S. A. Carr, T. J. Still, M. A. Blitz, A. J. Eskola, M. J. Pilling, P. W. Seakins, R. J. Shannon, B. Wang and S. H. Robertson, *J. Phys. Chem. A*, 2013, **117**, 11142-11154.

6.   R. G. Gilbert and S. C. Smith, *Theory of Unimolecular and Recombination Reactions*, *Blackwell Scientific Publications*, 1990.

7.   J. R. Barker, *Int. J. Chem. Kinet.*, 2001, **33**, 232-245.

8.   S. J. Klippenstein and J. A. Miller, *J. Phys. Chem. A*, 2002, **106**, 9267-9277.

9.   J. A. Miller and S. J. Klippenstein, *J. Phys. Chem. A*, 2006, **110**, 10528-10544.

10. D. R. Glowacki, C. H. Liang, C. Morley, M. J. Pilling and S. H. Robertson, *J. Phys. Chem. A*, 2012, **116**, 9545-9560.

11. J. A. Miller and S. J. Klippenstein, *Phys. Chem. Chem. Phys.*, 2013, **15**, 4744-4753.

12. J. A. Miller, S. J. Klippenstein, S. H. Robertson, et al., *J. Phys. Chem. A*, 2016, 120, 306-312.

13. J. R. Barker, M. Frenklach and D. M. Golden, *J. Phys. Chem. A*, 2015, 119, 7451-7461.

14. R. Whitesides, A. C. Kollias, D. Domin, W. A. Lester, Jr. and M. Frenklach, *Proc. Combust. Inst.*, 2007, **31**, 539-546.

15. R. Whitesides, D. Domin, R. Salomón-Ferrer, W. A. Lester and M. Frenklach, *J. Phys. Chem. A*, 2008, **112**, 2125-2130.

16. R. Whitesides, D. Domin, R. Salomón-Ferrer, W. A. Lester Jr and M. Frenklach, *Proc. Combust. Inst.*, 2009, **32**, 577-583.

17. R. Whitesides and M. Frenklach, *J. Phys. Chem. A*, 2010, **114**, 689-703.

18. X. Q. You, R. Whitesides, D. Zubarev, W. A. Lester and M. Frenklach, *Proc. Combust. Inst.*, 2011, **33**, 685-692.

19. X. Q. You, D. Y. Zubarev, W. A. Lester and M. Frenklach, *J. Phys. Chem. A*, 2011, **115**, 14184-14190.

20. D. E. Edwards, X. Q. You, D. Y. Zubarev, W. A. Lester Jr and M. Frenklach, *Proc. Combust. Inst.*, 2013, **34**, 1759-1766.

21. D. E. Edwards, D. Y. Zubarev, W. A. Lester and M. Frenklach, *J. Phys. Chem. A*, 2014, **118**, 8606-8613.

22. R. I. Singh, A. M. Mebel and M. Frenklach, *J. Phys. Chem. A*, 2015, **119**, 7528-7547.

23. X. You, H. Wang, H.-B. Zhang and M. J. Pilling, *Phys. Chem. Chem. Phys.*, 2016, **18**, 12149-12162.

24. H. Wang and M. Frenklach, *Combust. Flame*, 1994, **96**, 163-170.

25. J. T. Bartis and B. Widom, *J. Chem. Phys.*, 1974, **60**, 3474-3482.

26. M. J. Pilling and S. H. Robertson, *Annu. Rev. Phys. Chem.*, 2003, **54**, 245-275.

27. M. J. Pilling, *J. Phys. Chem. A*, 2013, **117**, 3697-3717.

28. A. Raj, G. R. da Silva and S. H. Chung, *Combust. Flame*, 2012, **159**, 3423-3436.

29. R. Singh and M. Frenklach, *Carbon*, 2016, **101**, 203-212.

30. H. O. Pritchard, *Can. J. Chem.*, 1977, **55**, 284-292.

31. T. Baer and W. L. Hase, *Unimolecular reaction dynamics : theory and experiments*, *Oxford University Press*, 1996.

32. N. J. B. Green and S. H. Robertson, *Chem. Phys. Lett.*, 2014, **605**, 44-46.

33. D. R. Glowacki, J. Lockhart, M. A. Blitz, S. J. Klippenstein, M. J. Pilling, S. H. Robertson and P. W. Seakins, *Science*, 2012, **337**, 1066-1069.